# Synthesis of Selenium Sulfide Nanoparticles in Polysaccharide Arabinogalactan and Starch Matrices

**M. V. Lesnichaya[a],\* and B. G. Sukhov[a]**

[a] *Favorsky Irkutsk Institute of Chemistry, Siberian Branch, Russian Academy of Sciences, Irkutsk, Russia*
*\*e-mail: mlesnichaya@mail.ru*

**Abstract**—New water-soluble $SeS_2$ containing nanocomposites are obtained via ion-exchange interaction between selenous acid and ammonium sulfide in water using natural arabinogalactan and starch polysaccharides as nanoparticle stabilizers. The transmission electron microscopy, X-ray diffraction analysis, and dynamic light scattering data show that nanocomposites are formed as spherical crystalline $SeS_2$ nanoparticles 5−140 nm in size, dispersed in polysaccharide matrices. The type of stabilization matrix and ratio of reactants have a decisive influence on the nanomorphological properties of the materials obtained.

## INTRODUCTION

The development of effective methods for synthesizing new promising nanomaterials and the search for potential areas of their use have attracted much attention over the past decade [1−3]. The main reason for this are the qualitatively new properties of materials or their manifold improvement during their structural modification from the bulk state to the nanoscale one [4, 5].

The creation of new effective materials is particular in demand in biomedicine [6] and optoelectronics [7]. Selenium [8] and sulfur [9] nanoparticles having high potential for the use in these areas are widely studied above any other objects. Indeed, selenium nanoparticles ($Se^0$ NPs) have the lowest toxicity among all organic and inorganic selenium compounds and possess antioxidant, antitumor, antimicrobial, antiinflammatory, and other activity [10−13]. A particular biological activity and the toxicity of $Se^0$ NPs depend on a size. This makes it possible to regulate their action by varying the size of NPs [14].

Similar results were obtained for sulfur nanoparticles ($S^0$ NPs) used as antibacterial and chemotherapeutic agents [9, 15]. These NPs have been used successfully in optoelectronics as cathode materials in high-performance lithium-ion batteries [16−18].

Selenium sulfide is a substance that possesses the biological and electronic properties of both selenium and sulfur. Extensive use of selenium sulfide in the biomedicine (namely, in dermatology) is due to its fungicidal and cytostatic (antimitotic) effects [19]. It is an antifungal agent against *Malassezia furfur*, *Microsporum sp.*, *Microsporum audouinii*, *Microsporum canis*, *Pityrosporon sp.*, *Trichophyton sp.*, *Trichophyton schoenleinii*, and *Trichophyton tonurans*. In addition, selenium sulfide decreases the growth of hyperproliferative cells in seborrhea and the production of epidermal and follicular epithelial corneocytes [20]. $SeS_2$ nanoparticles possess almost all bulk/$SeS_2$ antifungal activities and have higher conductivity in contrast to $Se^0$ or $S^0$ NPs. This makes it possible to obtain batteries with a high throughput, extremely stable cycle (up to 2000 cycles), and excellent capacity [21, 22].

The chemical methods occupy a central position among any other one to synthesize $SeS_2$. They imply the interaction between Se and S precursors in the presence of a stabilizer. The main advantages of these methods are the absence of special expensive hardware, the availability of reagents used, easy standardization, high reproducibility, and the absence of the need for additional purification of resulting nanomaterials from unreacted residues and microbiological by-products, as in the case of preparation of $SeS_2$ NPs from plant extracts or microorganisms [23−25].

An approach based on the ability of natural arabinogalactan (AG) and starch (St) polysaccharides to stabilize various surfaces of NPs is used in this work to synthesize the $SeS_2$ NPs. In this case, a single hybrid water-soluble organic-inorganic "core ($SeS_2$ NPs)/shell (polysaccharide matrix)" system is formed. In particular, water-soluble aggregatively stable nanocomposites ($Ag^0$, $Au^0$, $Fe_3O_4$, $Pd^0$, $Se^0$, and any other nanoparticles stabilized with AG and St) were obtained based on this approach [26−31].

The stabilization agents (AG and St) are available natural water-soluble polysaccharides. They are

widely used in the food and pharmaceutical industries and possess their own biological activities (immuno-modulatory, membranotropic, anti-inflammatory, hypolipidemic, and detoxification one) [32]. The incorporation of $SeS_2$ NPs into the AG and St polysaccharide matrices will make it possible to obtain materials that combine all these polysaccharide properties together with valuable biological and optical properties of $SeS_2$.

The preparation of particles in the necessary size range seems to be a main criterion to assess the possibility of their further use due to the decisive influence of the NPs' size on their physicochemical and biological properties. The size of particles formed depends on the preparation conditions. Its control, therefore, is possible by varying the synthesis conditions, including the type of a stabilizer and the quantitative ratio of reagents.

The aim of this work is to develop the optimal conditions to synthesize selenium sulfide nanoparticles in the stabilization arabinogalactan and starch matrices to assess the degree of their influence on the nanomorphological characteristics of the materials obtained.

## EXPERIMENTAL

AG from Siberian larch (*Larix Sibirica*) was used in this work. AG was extracted and purified according to the procedure described in [33]. The molecular weight of AG found earlier with a high performance liquid chromatography was 42.3 kDa [27]. 20% $(NH_4)_2S$ aqueous solution (Sigma Aldrich), $H_2SeO_3$ (Vekton), water-soluble starch (Reakhim), and ethanol (Reakhim) were used without additional purification. The average viscosity molecular weight of starch found with a viscometric method based on its 0.005% aqueous solution according to the method described in [34] was 326 kDa.

IR spectra were acquired in KBr within the $4000-400$ $cm^{-1}$ frequency range on a Varian Resolutions Pro spectrometer. KBr in an amount of 800 mg was ground and mixed thoroughly with 4 mg of the analyzed sample, after which the mixture was pressed into a tablet with $0.93-0.94$ mm in thickness on a Dezimalpresse DP 36 press at a pressure of 170 kgf $cm^{-2}$ before IR measurements.

X-ray diffraction analysis was performed on a Bruker D8 ADVANCE diffractometer equipped with a Goebbel mirror under Cu radiation in the locked Coupled mode with an exposure of 1 s for the phase analysis and 3 s to calculate the cell parameters and the size of a coherent scattering region.

Absorption spectra of 0.2% aqueous solutions of $SeS_2$ containing nanocomposites based on AG and St were recorded relative to distilled water in a 1 cm quartz cell in the $190-1000$ nm wavelength range on a UNICO 2800 UV/VIS spectrophotometer.

The micrographs of the samples were obtained on a Leo 906 E transmission electron microscope. 2–3 mg of a sample analyzed was dissolved in water for microscopic measurements. The solutions were diluted until the optical density of the final solution was 0.1. A drop of the resulting nanocomposite solution was placed on a formvar substrate film with subsequent drying in air and microscopic measurement. An IPWin45 software was used to measure the size of particles. The distribution of NPs was obtained with a statistical processing of at least seven micrographs of different areas of the analyzed substrate to obtain the data on size of $900-1000$ particles.

Elemental analysis (EA) was performed with X-ray energy dispersive microanalysis on a Hitachi TM 3000 scanning electron microscope equipped with an SDD XFlash 430-4 X-ray detector and on a Thermo Scientific Flash 2000 CHNS analyzer.

The hydrodynamic radii ($R_h$) of the $SeS_2$ NPs and macromolecules of the starting AG and St were found via dynamic light scattering (DLS) on a Photocor Compact-Z correlation spectrometer (the light source was a thermostabilized semiconductor laser with a power of 20 mW and a wavelength of $\lambda = 638$ nm) at an angle of 90°. The autocorrelation function was analyzed with a Dynals data processing program. The $R_h$ values were calculated from the diffusion coefficients ($D$) according to the Einstein−Stokes equation: $R_h = kT/6\pi\eta_0D^*$ ($\eta_0$ is the solvent viscosity, $k$ the Boltzmann constant, and $T$ the temperature). The solutions for the analysis were prepared via dilution of 0.5 ml of the reaction mixture in 2 ml of distilled water previously filtered through a syringe filter, after which the resulting diluted solution was again purified via filtration through a syringe filter (0.22 μm). The measurement time was at least 200 s. The measurement was repeated three times.

### Synthesis Procedure for SeS₂ Containing Nanocomposites

Five milliliters of an aqueous solution containing $0.16-0.82$ mmol $H_2SeO_3$ was added to a solution of AG or St (1.0 g in 50 ml of $H_2O$) at room temperature under vigorous stirring. Then the mixture was heated up to 40°C and stirred for 15 min. $51-254$ μL of $(NH_4)_2S$ solution was then added dropwise to the reaction mixture. The solution acquired a yellow-orange color. The synthesis time of nanocomposites was 30 min under constant stirring and at a temperature of 45°C. The $SeS_2$ containing nanocomposites were isolated and purified via precipitation of the reaction mixture cooled to room temperature in a fourfold excess of ethanol. The precipitate was repeatedly washed with ethanol on a filter, filtered off, and dried in air. The resulting nanocomposites were water-soluble red-orange powders with a yield of 92–95% and an selenium sulfide with a yield of $2.05-12.0\%$.
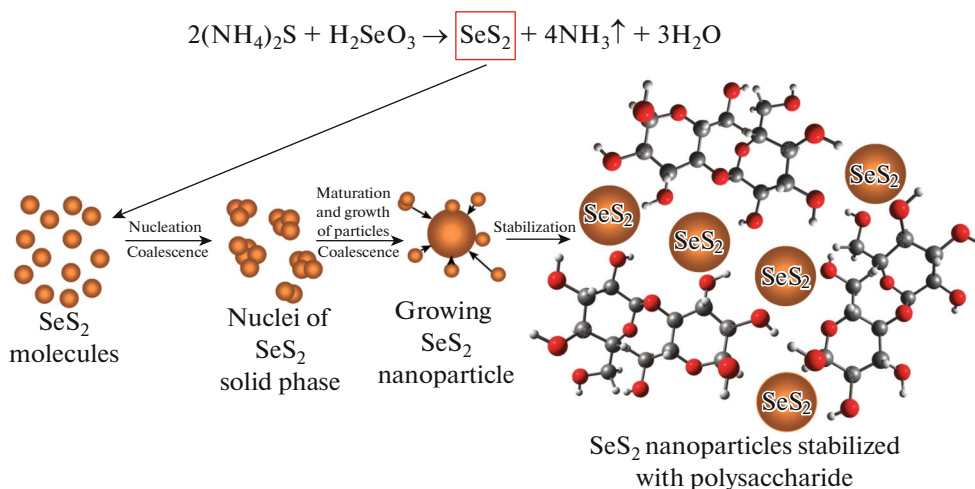
$$2(NH_4)_2S + H_2SeO_3 \rightarrow \boxed{SeS_2} + 4NH_3\uparrow + 3H_2O$$



**Fig. 1.** (Color online) Proposed scheme for synthesis of SeS$_2$ nanoparticles stabilized with polysaccharide.

The elemental composition was a follows (found in %): for AG, H 6.1 and C 41.5; for SeS$_2$/AG (2.05% SeS$_2$): H 5.7, C 42.0, Se 1.2, and S 0.85; for SeS$_2$/AG (6.0% SeS$_2$): H 5.14, C 40.0, Se 3.3, and S 2.67; for SeS$_2$/AG (12.0% SeS$_2$): H 5.35, C 41.97, Se 6.6, and S 5.35; for starch: H 6.4 and C 42.7; for SeS$_2$/St (2.07% SeS$_2$): H 5.57, C 41.87, Se 1.23, and S 0.87; for SeS$_2$/St (12.0% SeS$_2$): H 5.79, C 41.4, Se 6.5, and S 5.4. IR, KBr ($v^{-1}$), for AG: 3422 (O−H), 2920 (C−H), 1642 (O−H of adsorbed water), and 886−1216 cm$^{-1}$ (C−O antisymmetric oscillations of C−O−H and C−O−C groups); for starch: 3433 (O−H), 2928 (C−H), 1637 (O−H of adsorbed water), 1080, 1021, and 931 cm$^{-1}$ (oscillations of C−H, C−O, and C−C bonds of *D*-glucopyranose ring).

## RESULTS AND DISCUSSION

The SeS$_2$ nanoparticles were synthesized via the ion-exchange interaction between aqueous solutions of ammonium sulfide and selenous acid in aqueous solution of St and AG polysaccharide matrices (Fig. 1).

This reaction leads to selenium sulfide molecules with their subsequent combination and crystallization into NPs. The formation process of NPs proceeds through many stages, the first of which is the formation of SeS$_2$ molecules [35]. SeS$_2$ is formed in the reaction medium theoretically completely by the end of the first process stage due to the high rates of ion exchange reactions. When the critical concentration of SeS$_2$ molecules in the reaction medium is reached, the process of their coalescence starts to form nuclei of a new inorganic solid phase with their subsequent growth and maturation to SeS$_2$ NPs. The main factor that determines the rate of these processes is the diffusion of SeS$_2$ molecules to the surface of a growing NP. The

diffusion depends on the molecular weight and the viscosity properties of the polysaccharides being in the reaction medium.

The passivation of the energy-saturated surface of SeS$_2$ NPs and their aggregation stability proceed due to the adsorption of AG and St polysaccharide macromolecules on their surface (steric stabilization) and the electrostatic stabilization of the NP surface by highly polar hydroxyl, terminal, and carbonyl functional groups of AG and St polysaccharide macromolecules. In this case, a single hybrid stable water-soluble nano-core (SeS$_2$ NPs)/polysaccharide matrix system is formed.

X-ray diffraction analysis (XRD) data show that all the nanocomposites obtained are amorphous-crystalline substances. Their diffraction patterns have a halo of the amorphous phase of AG and St biopolymer matrix and a set of broadened reflections with various intensities within $2\theta = 14-29°$ assigned to the SeS$_2$ nanocrystalline particles (Fig. 2a). The average sizes of SeS$_2$ crystallites calculated according to the Debye−Scherrer formula vary within 9.2−69.4 nm depending on a type of a stabilizer and their amount in the composite (Table 1).

A significant decrease in intensity of the reflections and their broadening in comparison with the intense narrow reflections of the SeS$_2$ powder sample synthesized for comparison indicate probably that selenium sulfide particles in the nanocomposite have small size. In addition, the localization of reflections of SeS$_2$ NPs in the $2\theta$ location of a halo of the amorphous phase of a polysaccharide can influence their intensity.

Transmission electron microscopy (TEM) data show that the SeS$_2$ containing nanocomposites are formed as selenium sulfide nanoparticles dispersed in AG and St matrices, whose size varies within 5−140 nm and their shape is close to spherical (Figs. 3
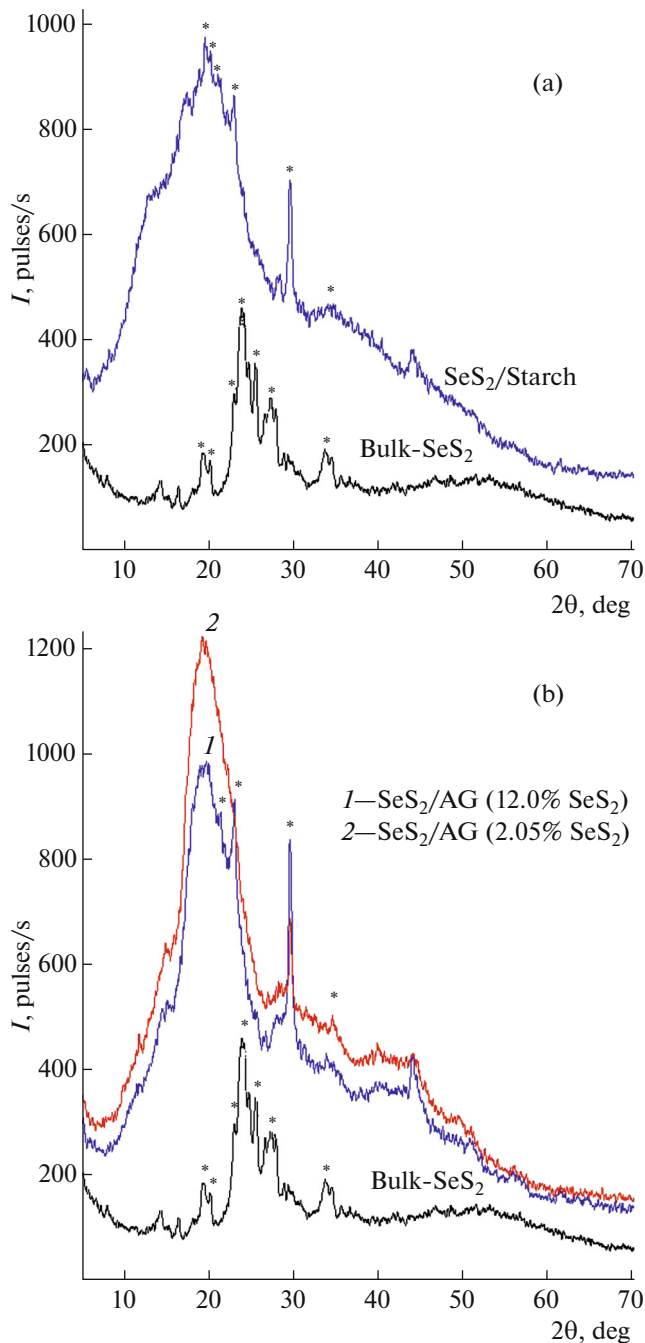
**Fig. 2.** (Color online) X-ray diffraction patterns of SeS$_2$ containing nanocomposites based on: (a) starch and (b) arabinogalactan with different amount of SeS$_2$ nanoparticles.

and 4). Their average size and the degree of polydispersity depend on the synthesis conditions for nanocomposites.

We found that the particles with the smallest size (5−15 nm) were formed, when St was used as a stabilization matrix in the case of a low amount of SeS$_2$ NPs (2.05%). The average size of SeS$_2$ NPs was 8 nm

in this case. An increase in quantitative amount of SeS$_2$ in the starch matrix to 12.0% leads to a broadening of the polydispersity of selenium sulfide particles (34−140 nm) and an increase in their average size up to 65 nm. The AG macromolecules used as a stabilizer lead to the SeS$_2$ NPs in the nanocomposites with an average size of 26 and 39 nm, which contain 2.07 and 12.0% of SeS$_2$, respectively. The trend towards an increase in the polydispersity and the average size of SeS$_2$ NPs in the case of AG also remains unchanged, but it is less pronounced than that of starch as a stabilizer (Table 1).

The DLS method was used to study the dynamics of the synthesis of SeS$_2$ NPs in the AG and St polysaccharide matrices. This was performed to discover the influence of a type of polysaccharide matrix, the duration of synthesis, and the ratio of precursors on dimensional characteristics of the resulting NPs. The data show that the initial AG solution has a bimodal distribution of scattering intensities with maxima corresponding to $R_h$ values of 8.3 and 50.1 nm. On the other hand, the distribution of particles not by the intensity, but by their number has a monomodal type with a maximum corresponding to $R_h$ = 9.6 nm (Fig. 5a). The type of a light scattering intensity distribution depends strongly on the degree of polydispersity of the sample [36, 37], the size and shape of the particles, and the presence of random large particles in the volume of the sample analyzed [36, 38]. Taking these data into account, the maximum at $R_h$ = 8.3 nm (9.6 nm in the case of a distribution by number of particles) corresponds probably to the hydrated individual AG macromolecules. The fact that there is no a maximum at $R_h$ = 50.1 nm in the case of a distribution by number of particles indicates probably that there is a low amount of aggregates of AG macromolecules in the aqueous solution, which make a significant contribution to the total scattering intensity of the sample. Their number, however, is negligible compared to individual poorly scattering AG macromolecules. Similar pattern is observed in the case of the starch aqueous solution. Its initial solution in the distribution of scattering intensity leads to two maxima corresponding to $R_h$ of particles to be 17.7 and 126.3 nm, which are probably assigned to the individual macromolecules and the aggregated forms of starch, respectively, as in the case of AG. In the case of a distribution by number of particles, the second maximum disappears and only one remains, which corresponds to $R_h$ = 22.6 nm (Fig. 5b). This clear difference in the position and the number of maxima, that characterize the dispersion of particles in the samples, when the distribution of the number of particles is used instead of by the scattering intensity, indicate that the distribution of particles and their $R_h$ should be further characterized by the number of particles. This will minimize the influence of random highly scattering large particles (or aggregates) on the data obtained.

The introduction of an aqueous solution of selenous acid into AG or St shifts the pH of the reaction medium to the acidic region. An increase in mass ratio of polysaccharide : $H_2SeO_3$ from 1 : 47 to 1 : 10 leads to a more intense decrease in pH from 4.5 to 3.0. Conversely, the addition of $H_2SeO_3$ to AG and St increases the ionic strength of the solution. The anionic additives, taking into account the polyelectrolyte nature of the polysaccharides used, can affect the intensity of intermolecular interactions [39, 40], which in this case was confirmed by a slight decrease in $R_h$ value of starch to 19.1 nm and AG to 8.4 nm. This was probably due to a partial conformational transition of straightened AG and St macromolecules in a neutral medium into a more compact coil form owing to ionization of their polar groups [40]. An insignificant decrease in $R_h$ of particles during acidification of the medium agrees well with the published data and is characteristic of the pH range 2.3–7.0 in contrast to a sharp decrease in $R_h$ with an increase in pH [40–42]. The addition of ammonium sulfide to the mixture of polysaccharide and selenous acid leads to the retention of the dispersed monomodal distribution by the number of particles and an increase in $R_h$ with an increase in the synthesis time from 0 to 30 min. Indeed, the $R_h$ of the particles in the reaction medium increases insignificantly

**Table 1.** Average diameters ($d$) of $SeS_2$ nanoparticles in arabinogalactan (AG) and starch (St) matrices obtained with TEM, XRD, and DLS

| Sample | $d$, nm TEM | $d$, nm XRD | $d$ ($2R_h$), nm DLS |
|---|---|---|---|
| $SeS_2$/AG (2.05%) | 26 | 24.7 | 123.9 |
| $SeS_2$/AG (12.0%) | 39 | 43.6 | 146.5 |
| $SeS_2$/St (2.07%) | 8 | 9.2 | 104.7 |
| $SeS_2$/St (12.0%) | 65 | 69.4 | 205.0 |

to 22.6 nm immediately after ammonium sulfide at a concentration of 0.000022 mol is introduced into the starch–selenous acid mixture. The average $R_h$ value of the particles also increased to 31.6, 37.3, 44.2, and 52.3 nm at 3, 7, 20, and 30 min of the synthesis process, respectively, with an increase in the duration of synthesis (Fig. 6a). An increase in the concentration of $H_2SeO_3$ and $(NH_4)_2S$ to 0.000032 and 0.000065 mol, respectively, during synthesis of the nanocomposite also led to an increase in $R_h$ of particles from 28.4 to 37.2, 58.7, 86.7, and 102.5 nm at 0, 3, 7, 20, and 30 min of the synthesis process, respectively (Fig. 6b). When the duration of synthesis increased to 40 min, there
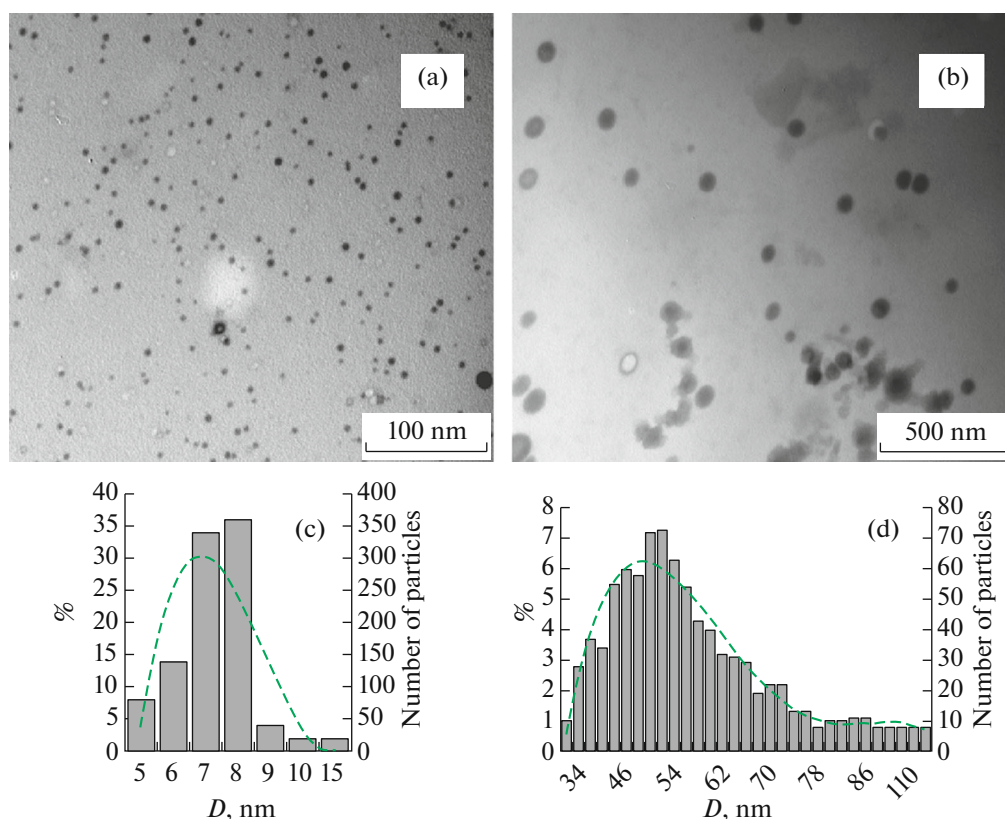


Fig. 3. (Color online) Micrographs and dispersed distribution of $SeS_2$ nanoparticles in starch polysaccharide matrix with their amount of: (a, c) 2.07 and (b, d) 12.0%.
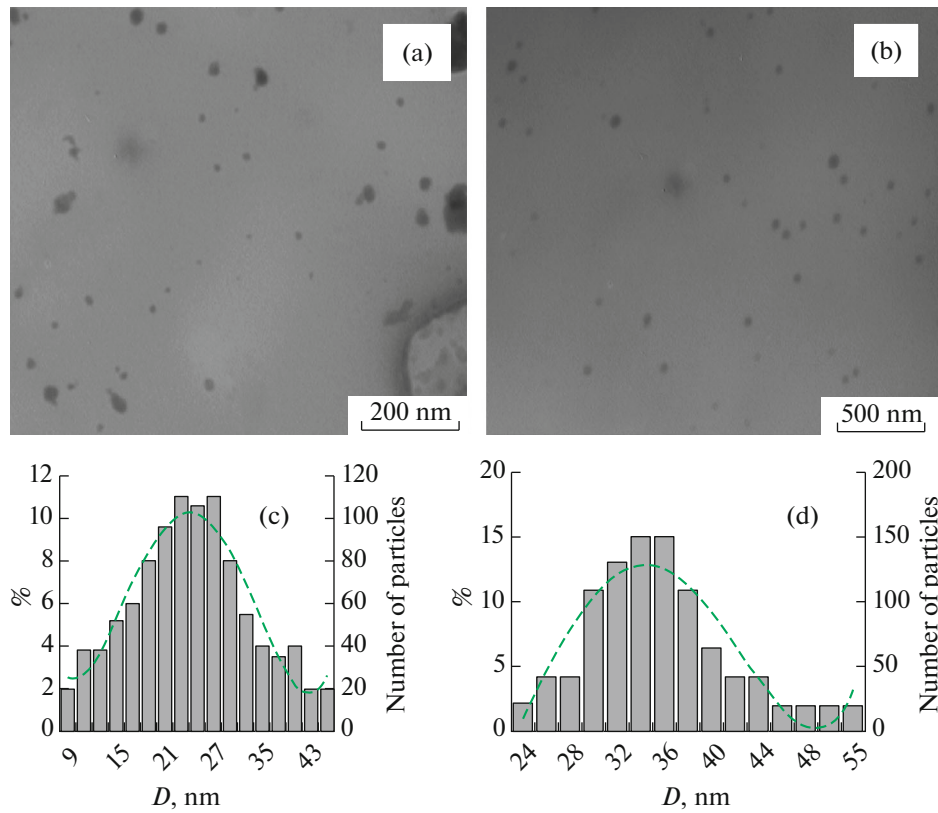
**Fig. 4.** (Color online) Micrographs and dispersed distribution of SeS$_2$ nanoparticles in arabinogalactan polysaccharide matrix with their amount of: (a, c) 2.05 and (b, d) 12.0%.
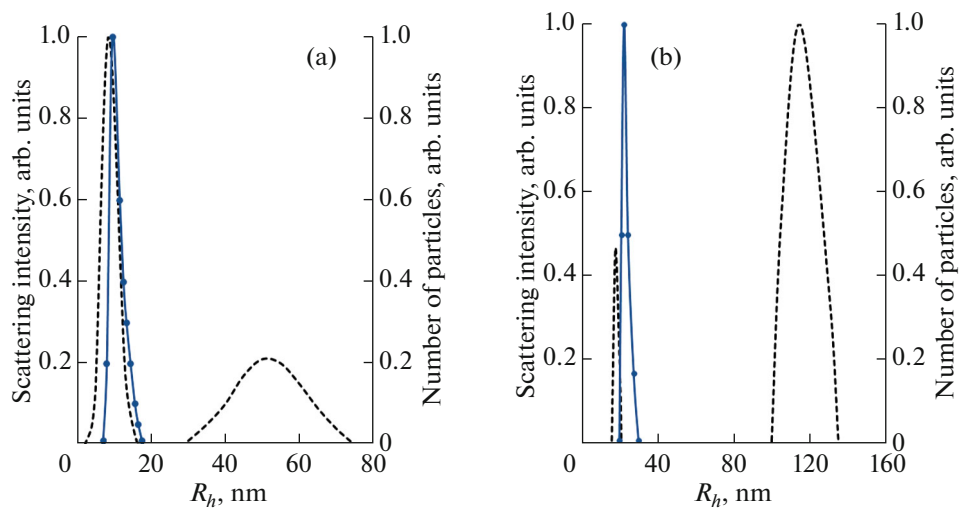


**Fig. 5.** (Color online) Distribution of (dashed line) scattering intensity and (solid line) the number of scattering particles for: (a) arabinogalactan and (b) starch.

was no significant change in $R_h$, which probably indicated completion of the stabilization process of SeS$_2$ NPs to form the nanocomposite.

When AG was used as a stabilizer, the addition of ammonium sulfide at a concentration of 0.000022 or 0.000065 mol to the reaction mixture increased the $R_h$ of particles to 25.4 and 31.6 nm, respectively. An increase in the synthesis time to 3, 10, and 30 min led to a gradual increase in $R_h$ of particles (for high concentrations of precursors) to 44.2, 61.9, and 73.2 nm,
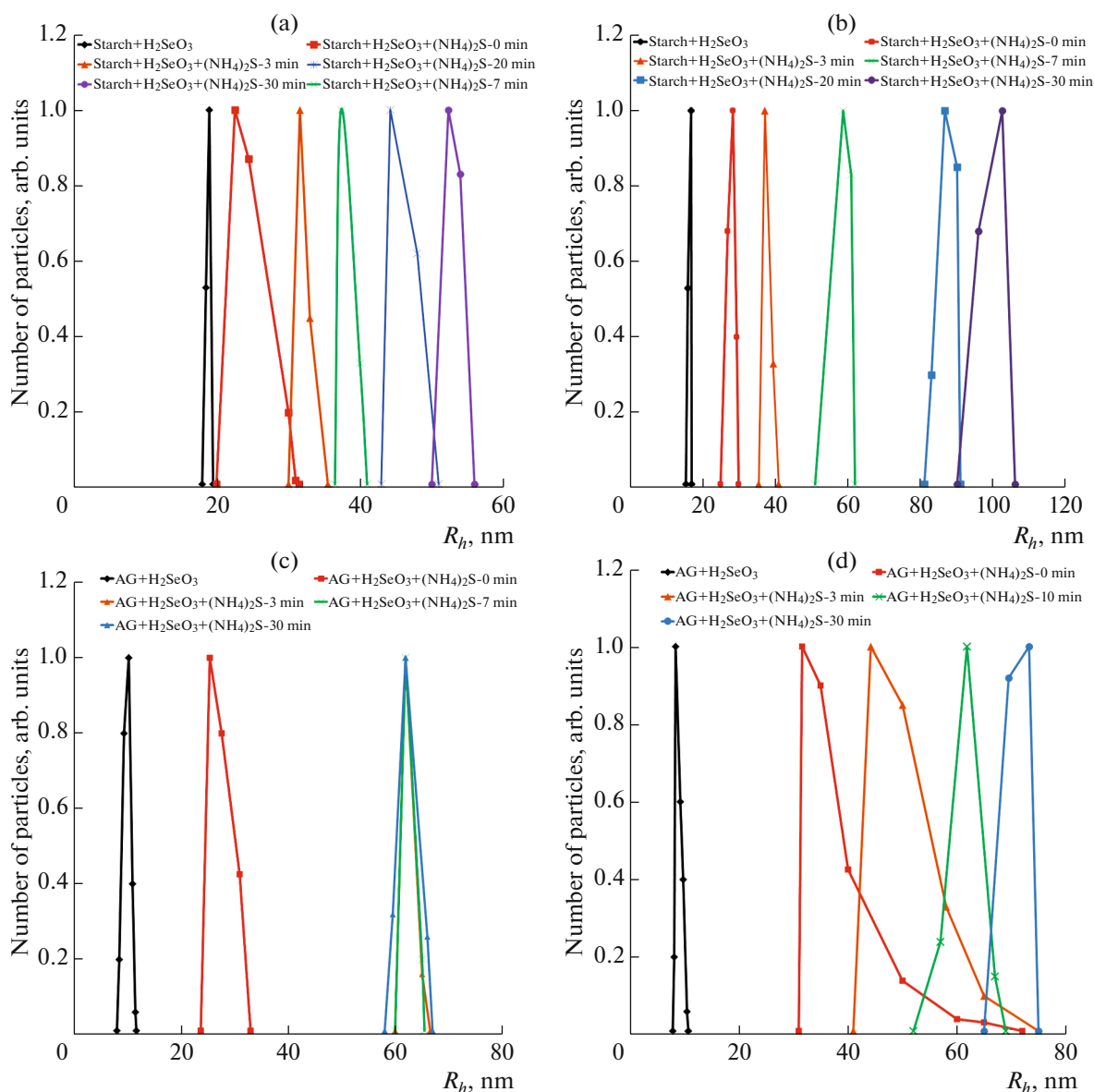
**Fig. 6.** (Color online) Dynamics of changes in hydrodynamic radius of particles during the synthesis of $SeS_2$ containing nanocomposites based on (upper row) starch and (lower row) arabinogalactan under different quantitative amount of precursors: (a, c) 0.000011 mol of $H_2SeO_3$ and 0.000022 mol of $(NH_4)_2S$ or (b, d) 0.000032 mol of $H_2SeO_3$ and 0.000065 mol of $(NH_4)_2S$.

respectively (Fig. 6d). Conversely, there was no change in $R_h$ starting from the third minute of synthesis at low concentrations of selenous acid and ammonium sulfide. The values obtained were 61.9, 61.9, and 61.9 nm at 3, 7, and 30 min of the synthesis process (Fig. 6c). This suggests possible completion of the stabilization process and the formation of $SeS_2$ NPs by AG macromolecules at the third minute of the synthesis, with their low amount (2.05%) in the bulk of the polysaccharide matrix. In the case of high concentrations of a precursor, the aggregation processes of the $SeS_2$ NPs also proceed together with the formation of the $SeS_2$ NPs (chemical ion exchange between sele-

nous acid and ammonium sulfide, the formation of solid phase nuclei, and the coalescence and surface stabilization) possibly with the subsequent dissolution of some aggregates formed. In this case, the mobility of AG macromolecules can be decreased in an aqueous solution at a higher ionic strength, which generally increases the time required to complete synthesis of the $SeS_2$/AG nanocomposite.

It should be noted that $R_h$ corresponds to the hydrodynamic radius of the particles in the bulk solution and characterizes the size of not only $SeS_2$ NPs, but also of the shell covering the NP surface of hydrated polysaccharide macromolecules. The ability
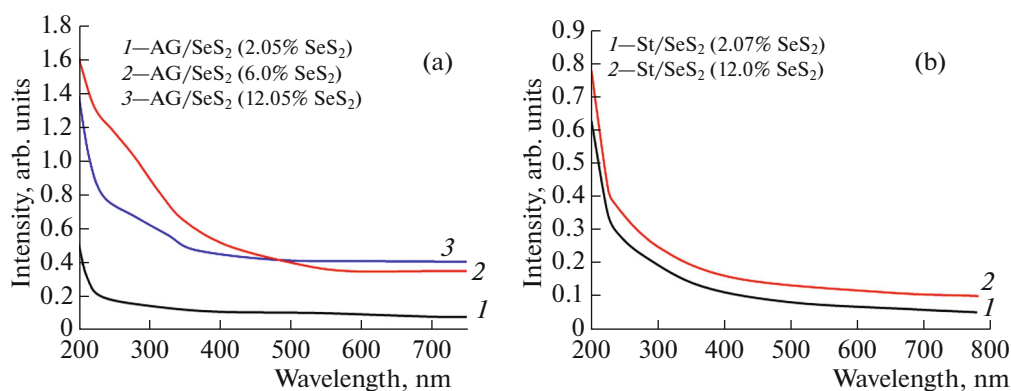
**Fig. 7.** (Color online) Absorption spectra of aqueous solutions of $SeS_2$ containing nanocomposites based on: (a) arabinogalactan and (b) starch with different amount of $SeS_2$ nanoparticles.

of polysaccharide to the solvation, which depends on the structure of a macromolecule, the degree of polymerization, molecular weight, temperature, and the ions present in the solution, influences significantly the $R_h$ value. We may assume that the $R_h$ value found with DLS method is probably assigned to polysaccharide-stabilized $SeS_2$ NPs, rather than to their aggregates taking into account the size of $SeS_2$ NPs found with TEM, the spherical shape of all NPs, and the absence of massive aggregation of NPs in micrographs together with the narrowest dispersion distribution (by the time of the end of synthesis). In this case, the size of the hydrated shells of AG and St, which cover the NP surface, is the difference between the $2R_h$ value found with DLS method and the diameter of the $SeS_2$ NPs found from the TEM data. The resulting value varies within 98.0−107.5 nm for AG-based nanocomposites and 96.7−140.0 nm for starch-based one. The calculated data are in good agreement with the fact that the water-holding capacity of starch is high and that it is hygroscopic.

The absorption spectra of aqueous solutions of $SeS_2$ containing nanocomposites based on AG and St in the UV and visible regions of the spectrum are inexpressive (Fig. 7). Significantly high background absorption observed in the spectra of the AG-based nanocomposites confirms the TEM data, according to which rather large $SeS_2$ particles appear in this matrix. The spectra of $SeS_2$/St nanocomposites have the background absorption, but its intensity is less than that of $SeS_2$/AG nanocomposites. Generally, the pattern of the electronic absorption spectra of the $SeS_2$ containing nanocomposites is in good agreement with the data [23−25]. This, together with the XRD, TEM, DLS, and elemental analysis data, indicate that the $SeS_2$ NPs are successfully generated in the matrices of AG and St natural biopolymers, which stabilize their surface and provide the water solubility and the stability of the resulting nanocomposites.

## CONCLUSIONS

Hybrid organo-inorganic water-soluble nanocomposites based on arabinogalactan and starch that contain $SeS_2$ nanoparticles as an inorganic phase in an amount of 2.05 to 12.0% were synthesized for the first time. The quantitative ratio of the reactants and the stabilizer has the significant influence on the dimensional characteristics of selenium sulfide nanoparticles. The stabilization ability of AG and St polysaccharides depends on the quantitative amount of selenium sulfide introduced into their composition due to the influence of the pH and ionic strength of the solution on the conformation of their macromolecules in the solution of the reaction medium. High saturation of the reaction medium with precursor and by-product ions of the reaction during the synthesis of nanocomposites increases the polydispersity of the resulting nanocomposites and increases the size of the $SeS_2$ NPs formed.

## REFERENCES

1. M. D. Mauricio, S. Guerra-Ojeda, P. Marchio, et al., Oxid. Med. Cell. Longev. **2018**, 1 (2018).
https://doi.org/10.1155/2018/6231482

2. Z. Salman, U. Irshad, K. Ali, et al., Nanoscale Rep. **2**, 32 (2019).
https://doi.org/10.26524/nr1924

3. L. A. Kolahalam, I. V. K. Viswanat, B. S. Diwakar, et al., Mater. Today: Proc. **18**, 2182 (2019).
https://doi.org/10.1016/j.matpr.2019.07.371

4. A. Taloni, M. Vodret, G. Costantini, and S. Zapperi, Nat. Rev. Mater. **3**, 211 (2018).
https://doi.org/10.1038/s41578-018-0029-4

5. J. L. Rodriguez-Lopez, J. M. Montejano-Carrizales, J. P. Palomares-Baez, et al., Key Eng. Mater. **444**, 47 (2010).
https://doi.org/10.4028/www.scientific.net/KEM.444.47

6. A. P. Ramos, M. A. E. Cruz, C. B. Tovani, and P. Ciancaglini, Biophys. Rev. **9**, 79 (2017).
https://dx.doi.org/10.1007%2Fs12551-016-0246-2

7. S. Glebska, A. Szczecinska, N. Znajdek, et al., Acta Innov. **30**, 5 (2019).
http://dx.doi.org/10.32933%2FActaInnovations.30.1

8. L. M. Sosedova, V. S. Rukavishnikov, B. G. Sukhov, G. B. Borovskii, E. A. Titov, M. A. Novikov, V. A. Vokina, N. L. Yakimova, M. V. Lesnichaya, T. V. Kon'kova, M. K. Borovskaya, I. A. Graskova, A. I. Perfil'eva, and B. A. Trofimov, Nanotechnol. Russ. **13**, 290 (2018).

9. M. Suleiman, A. A. Ali, A. Hussein, et al., J. Mater. Environ. Sci. **5**, 1029 (2013).

10. S. Boroum, M. Safari, E. Shaabani, et al., Mater. Res. Express **6**, 211 (2019).
https://doi.org/10.1088/2053-1591/ab2558

11. M. Vahdati and T. T. Moghadam, Sci. Rep. **10**, 510 (2020).
https://doi.org/10.1038/s41598-019-57333-7

12. B. Hosnedlova, M. Kepinska, S. Skalickova, et al., Int. J. Nanomed. **13**, 2107 (2018).
https://dx.doi.org/10.2147%2FIJN.S157541

13. S. M. Amini and V. P. Mahabadi, Nanomed. Res. J. **3**, 117 (2018).
https://doi.org/10.22034/nmrj.2018.03.001

14. G. B. Sergeev, Ros. Khim. Zh. **46**, 22 (2002).

15. R. M. Tripathia, P. R. Rao, and T. Tsuzuki, RSC Adv. **8**, 36345 (2018).
https://doi.org/10.1039/C8RA07845A

16. S. Risse, E. Hark, B. Kent, and M. Ballauff, ACS Nano **13**, 10233 (2019).
https://doi.org/10.1021/acsnano.9b03453

17. H. Chen, C. Wang, W. Dong, et al., Nano Lett. **15**, 798 (2015).
https://doi.org/10.1021/nl504963e

18. R. Mo, Z. Lei, D. Rooney, and K. Sun, Energy Storage Mater. **23**, 284 (2019).
https://doi.org/10.1016/j.ensm.2019.04.046

19. P. R. Cohen and C. A. Anderson, Dermatol. Ther. (2018).
https://doi.org/10.1007/s13555-018-0259-9

20. F. Mavadnejad, F. Rafii, E. Faghfuri, et al., Am. Res. J. Dermatol. **1**, 22 (2013).

21. Z. Li, J. Zhang, Y. Lu, and W. X. Lou, Sci. Adv. **4**, 1 (2018).
https://doi.org/10.1126/sciadv.aat1687

22. J. He, W. Lv, and Y. Chen, J. Mater. Chem. A **22**, 1 (2018).
https://doi.org/10.1039/c8ta02434k

23. F. Asghari-Paskiabi, M. Imani, H. Rafii-Tabar, and M. Razzaghi-Abyaneh, Biochem. Biophys. Res. Commun. **516**, 1078 (2019).
https://doi.org/10.1016/j.bbrc.2019.07.007

24. K. R. Raksha, S. Ananda, and R. Narayanaswamy, J. Sulfur Chem. **12**, 471 (2015).
https://doi.org/10.1080/17415993.2015.1057511

25. I. A. Kariper, S. Ozden, and F. M. Tezel, Opt. Quantum Electron. **50**, 441 (2018).
https://doi.org/10.1007/s11082-018-1693-8

26. T. V. Fadeeva, I. A. Shurygina, B. G. Sukhov, M. K. Rai, M. G. Shurygin, V. A. Umanets, M. V. Lesnichaya, T. V. Kon'kova, and D. M. Shurygin, Bull. Russ. Acad. Sci.: Phys. **79**, 273 (2015).

27. G. P. Aleksandrova, A. S. Boymirzaev, M. V. Lesnichaya, B. G. Sukhov, and B. A. Trofimov, Russ. J. Gen. Chem. **85**, 488 (2015).

28. G. P. Aleksandrova, L. A. Grishchenko, A. S. Bogomyakov, B. G. Sukhov, V. I. Ovcharenko, and B. A. Trofimov, Russ. Chem. Bull. **59**, 2318 (2010).

29. L. P. Feoktistova, G. P. Aleksrova, L. A. Grishchenko, et al., Nanotekhnika **20**, 31 (2009).

30. M. V. Lesnichaya, S. F. Malysheva, N. A. Belogorlova, I. A. Graskova, A. V. Gazizova, A. I. Perfilyeva, O. A. Nozhkina, and B. G. Sukhov, Russ. Chem. Bull. **68**, 2245 (2019).

31. K. Wongmanee, S. Khuanamkam, and S. Chairam, J. King Saud Univ. Sci. **29**, 547 (2017).
https://doi.org/10.1016/j.jksus.2017.08.007

32. E. N. Medvedeva, V. A. Babkin, and L. A. Ostroukhova, Khim. Rastit. Syr'ya, No. 1, 27 (2003).

33. G. F. Antonova and N. A. Tyukavkina, Khim. Drevesin., No. 2, 89 (1983).

34. P. Dokic, L. Dokic, T. Dapcevic, and V. Krstonosic, Prog. Colloid Polym. Sci. **135**, 48 (2008).

35. A. Yu. Olenin and G. V. Lisichkin, Russ. Chem. Rev. **80**, 605 (2011).

36. B. N. Khlebtsov and N. G. Khlebtsov, Colloid. J. **73**, 118 (2011).

37. R. Sadeghi, Z. Daniella, S. Uzun, and J. Kokini, J. Cereal Sci. **76**, 127 (2017).

38. E. R. Gasilova, A. A. Toropova, S. V. Bushin, et al., J. Phys. Chem. B **114**, 4204 (2010).

39. R. Pecora, *Dynamic Light Scattering: Applications of Photon Correlation Spectroscopy* (Plenum, New York, 1985).

40. A. Romdhane, M. Aurousseau, A. Guillet, and E. Mauret, Starch **67**, 319 (2015).

41. P. L. Russell and G. Oliver, J. Cereal Sci. **10**, 123 (1989).
https://doi.org/10.1016/S0733-5210(89)80041-4

42. E. Hosseini, H. R. Mozafari, M. Hojjatoleslamy, and E. Rousta, Food Sci. Technol. **37**, 1 (2017).
https://doi.org/10.1590/1678-457x.18116

*Translated by A. Tulyabaev*